

Pion-photon transition form factor in light-cone sum rules ¹

A. V. Pimikov^{*,†}, A. P. Bakulev[†], S. V. Mikhailov[†] and N. G. Stefanis^{**}

^{*}*Departamento de Física Teórica -IFIC, Universidad de Valencia-CSIC, E-46100 Burjassot (Valencia), Spain*

[†]*Bogoliubov Laboratory of Theoretical Physics, JINR, 141980 Dubna, Russia*

^{**}*Institut für Theoretische Physik II, Ruhr-Universität Bochum, D-44780 Bochum, Germany*

Abstract. We extract constraints on the pion distribution amplitude from available data on the pion-photon transition form factor in the framework of light-cone sum rules. A pronounced discrepancy $(2.7 - 3)\sigma$ between the Gegenbauer expansion coefficients extracted from the CELLO, CLEO, and Belle experimental data relative to those from BaBar is found. Predictions for the pion-photon transition form factor are presented by employing a pion distribution amplitude obtained long ago from QCD sum rules with nonlocal condensates. These predictions comply with the Belle data but disagree with those of BaBar beyond 9 GeV^2 .

Keywords: Transition form factors, pion distribution amplitude, higher twist, light-cone sum rules, collinear factorization, higher-order radiative corrections, renormalization-group evolution

PACS: 12.38.Lg, 12.38.Bx, 13.40.Gp, 11.10.Hi

PION-PHOTON TRANSITION FORM FACTOR IN LCSRS

The pion-photon transition $\gamma^* + \gamma^* \rightarrow \pi^0$ (see [1] for a review) is defined by the correlator of two electromagnetic currents

$$\int d^4z e^{-iq_1 \cdot z} \langle \pi^0(P) | T \{ j_\mu(z) j_\nu(0) \} | 0 \rangle = i \varepsilon_{\mu\nu\alpha\beta} q_1^\alpha q_2^\beta F^{\gamma^* \gamma^* \pi}(Q^2, q^2), \quad (1)$$

where $F^{\gamma^* \gamma^* \pi}(Q^2, q^2)$ is the pion-photon transition form factor (TFF) with the photon momenta q_1 and q_2 , and $Q^2 \equiv -q_1^2 > 0$, $q^2 \equiv -q_2^2 \geq 0$. This transition process was measured by the CELLO [2], CLEO [3], BaBar [4], and Belle [5] Collaborations for the kinematics $Q^2 \gg m_\rho^2$, $q^2 \ll m_\rho^2$ (the same also for the planned measurement by BESIII [6]). For this kinematics, perturbative QCD factorization is reliable only in the leading-twist approximation, while higher twists are also important as shown in [7]. For $q^2 < m_\rho^2$, one has to include the interaction of the (quasi) real photon at long distances $\sim O(1/\sqrt{q^2})$. To this end, we apply [8, 9] ² Light Cone Sum Rules (LCSR)s [18, 19] that effectively account for long-distance effects of the real photon making use of quark-

¹ Presented by the first author at the QCD@Work Conference, Lecce (Italy), 18–21 June, 2012.

² This contribution is based on our previous works [8, 9], where the detailed description of our LCSR application and the comparison of our results with some of other pion-photon TFF studies [10–17] can be found. Here, we only briefly describe the basic ingredients of our LCSR approach.

hadron duality in the vector channel and applying a dispersion relation in q^2 to get [19]

$$F_{\gamma\gamma^*\pi}(Q^2, q^2) = \int_0^{s_0} \frac{\rho^{\text{PT}}(Q^2, s)}{m_\rho^2 + q^2} e^{(m_\rho^2 - s)/M^2} ds + \int_{s_0}^\infty \frac{\rho^{\text{PT}}(Q^2, s)}{s + q^2} ds, \quad (2)$$

where $s_0 \simeq 1.5 \text{ GeV}^2$ is the effective threshold in the vector channel and M^2 is the Borel parameter $(0.7 - 0.9) \text{ GeV}^2$. The effect related to the small nonzero momentum q^2 was recently discussed in the framework of LCSRs [20], and also using Monte Carlo simulations [21]. Here, we neglect this effect and apply the real-photon limit $q^2 \rightarrow 0$ that can easily be taken in the LCSRs given by (2): $F_{\gamma\gamma^*\pi}(Q^2, q^2) \equiv F_{\gamma\gamma^*\pi}(Q^2, 0)$.

The spectral density has been calculated in QCD up to the level of the twist-six (Tw-6) term [15] (using similar notations for the other twists):

$$\rho^{\text{PT}}(Q^2, s) = \text{Im} F_{\gamma^*\gamma^*\pi}^{\text{PT}}(Q^2, -s - i\varepsilon) = \rho_{\text{Tw-2}} + \rho_{\text{Tw-4}} + \rho_{\text{Tw-6}} + \dots,$$

where the various twist contributions are given in the form of a convolution of the hard parts with the pion distribution amplitude (DA) of a given twist. At the same time, for the twist-two contribution we have the perturbative expansion

$$F_{\gamma^*\gamma^*\pi}^{\text{Tw-2}} \sim \left[T_{\text{LO}} + a_s(\mu^2) T_{\text{NLO}} + a_s^2(\mu^2) T_{\text{NNLO}_{\beta_0}} + \dots \right] \otimes \phi_\pi^{\text{Tw-2}}(x, \mu^2),$$

where $a_s = \alpha_s/4\pi$. In our studies all calculated terms have been included and they are shown in Fig. 1 as a chain of ovals each enclosing an area proportional to the absolute value of the corresponding contribution. The sum of all terms of each row gives its total contribution, as detailed in the accompanying table in this figure.

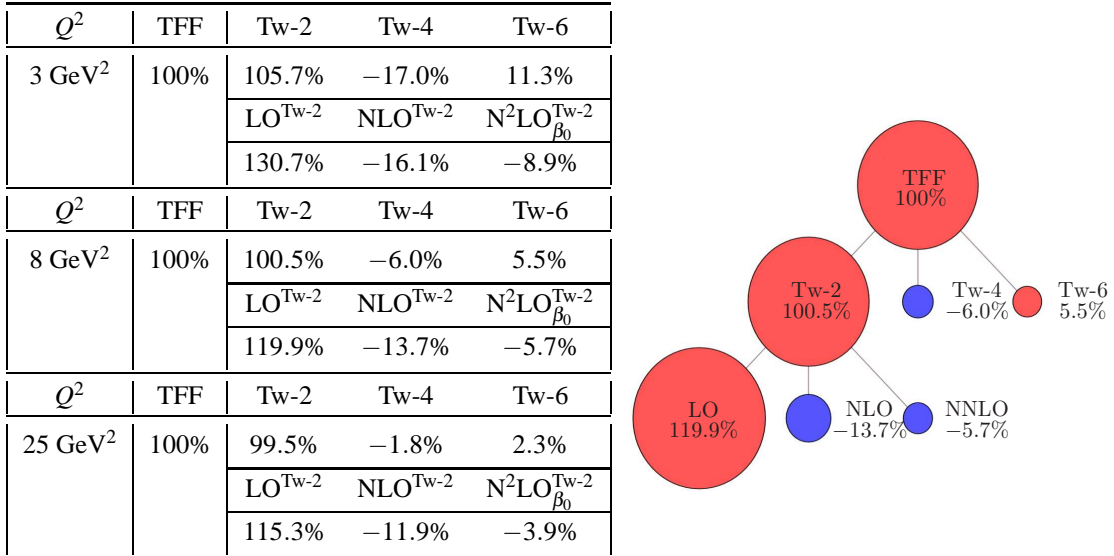


FIGURE 1. Relative percentage contributions to the pion-photon TFF $F_{\gamma\gamma^*\pi}(Q^2)$ with the asymptotic pion DA at $Q^2 = 3, 8$, and 25 GeV^2 in table form and graphically (shown only for $Q^2 = 8 \text{ GeV}^2$). The blue color corresponds to negative terms, while the red one denotes the positive terms.

As we see from Fig. 1, the twist-six contribution [15] and the next-to-next-to-leading order (NNLO) term [22] proportional to the β_0 -part have absolute values of similar

size but opposite signs in the whole Q^2 -region. Therefore, we consider their sum as a contribution to the theoretical uncertainties both for fitting the pion DA and for estimating the pion TFF for a given pion DA model. All other terms are included into the central value of the TFF: Leading order (LO), next-to-leading order (NLO) of twist-two [22] (corrected in [15]), and twist-four [19]. The uncertainties of the applied LCSR approach contain the sum of the NNLO twist-two and twist-six contributions, a 20% variation of the twist-four coupling $\delta^2(\mu^2) = 0.19 \text{ GeV}^2$ [23], and those uncertainties stemming from the pion DA model.

We consider the pion DA in terms of the first two coefficients³ of the full Gegenbauer expansion ($\bar{x} \equiv 1 - x$):

$$\phi_\pi(x, \mu^2) = 6x\bar{x} \left[1 + a_2(\mu^2)C_2^{3/2}(x - \bar{x}) + a_4(\mu^2)C_4^{3/2}(x - \bar{x}) + \dots \right].$$

The coefficients $a_n(\mu^2)$ are evolved according to the Efremov–Radyushkin–Brodsky–Lepage (ERBL) [24, 25] evolution equation to the NLO level [26].

Data analysis and predictions for the TFF

The described LCSR-based techniques allow the computation of the TFF for any pion DA given in the form of a Gegenbauer expansion. Using LCSRs with pion DAs obtained in QCD sum rules with nonlocal condensates [27], one obtains the predictions shown by a shaded (green) band in Fig. 2 in comparison with the available experimental data.

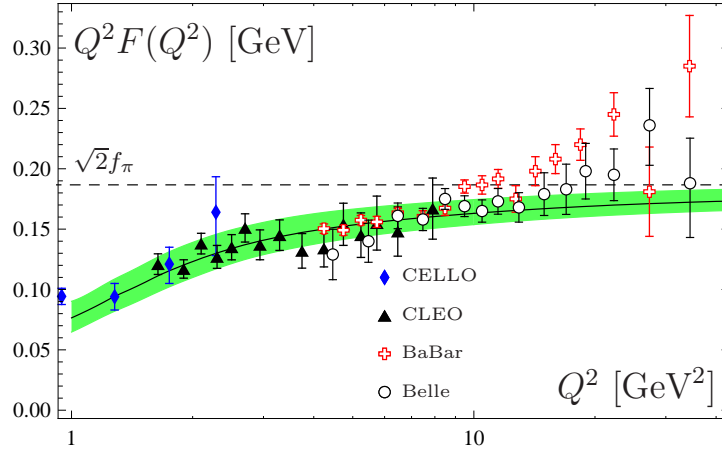


FIGURE 2. Theoretical predictions extracted in [8, 9] for the scaled $\gamma^* \gamma \pi^0$ TFF, calculated in the LCSR approach with pion DAs obtained in QCD sum rules with nonlocal condensates [27], in comparison with the experimental data from CELLO [2], CLEO [3], BaBar [4], and Belle [5].

On the other hand, one can fit the pion DA Gegenbauer coefficients to the different data sets in order to obtain corresponding experimental constraints. This can also reveal

³ The consideration of the pion in terms of three coefficients can be found in [8, 9].

the extent of the discrepancy among the various data sets. In Fig. 3, we present the confidential region of a_2 and a_4 given in the form of error ellipses derived from fitting different sets of data. Best-fit values of the χ -squared goodness of fit χ^2/ndf (ndf=number of degrees of freedom) are shown at the centers of the ellipses, while deviations between particular data sets are displayed on the sides of the triangle in units of one standard deviation ($1\sigma \approx 68\%$). From Fig. 3, we conclude that the inclusion of the BaBar data to those of CELLO&CLEO leads to a 3σ shifting of the confidential region from the (blue) ellipse at the bottom on the right to the (red) solid-lined ellipse at the top on the left, accompanied by a significant increase of the χ -squared goodness of fit value from 0.4 to 2. The additional inclusion of the Belle data plays no role in the two-parameter analyses (dashed-dotted (red) ellipse). If we include to the CELLO&CLEO data only the Belle data (ignoring the BaBar data), then the shifting of the confidential region is moderate (1.2σ), with a slight increase of the χ -squared goodness of fit value from 0.4 to 0.6 (dotted black ellipse). Note that we considered the χ -squared goodness of fit for the analyzed experiments, χ^2 , as the sum of the individual χ -squared goodness of fit values associated with each experiment. When the data strongly deviate from each other, this way of combining data could be inefficient for extracting the confidential region of the fitting parameters, though it is still good for identifying and rating this deviation.

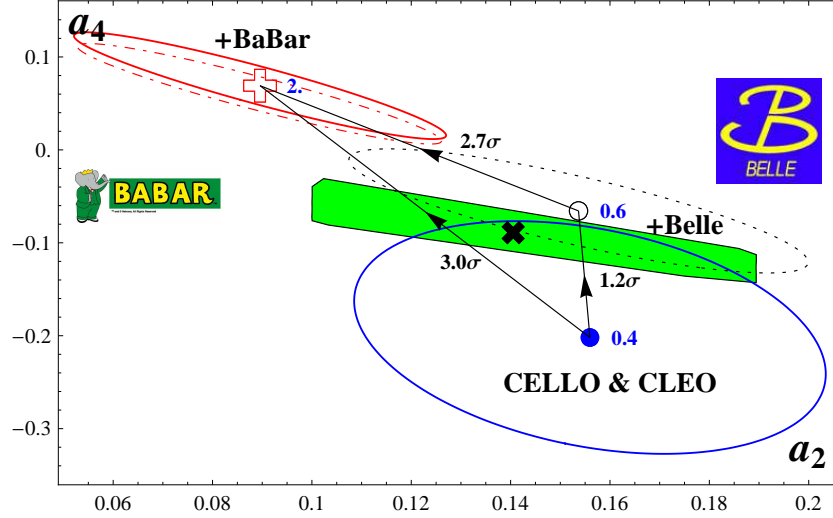


FIGURE 3. Confidential regions for two-parameter (a_2, a_4) fits based on three data sets: first - CLEO, CELLO [2, 3] (solid (blue) ellipse at the right bottom); second - CLEO, CELLO, and BaBar [4] (solid (red) ellipse at the left top); third - CLEO, CELLO, and Belle [5] (dotted ellipse at the center). Best fit values of the χ -squared goodness of fit χ^2/ndf are shown at the apexes of a triangle. On its sides we display the discrepancy among the data sets in terms of a standard deviation ($1\sigma \approx 68\%$). The area of the a_2, a_4 values allowed by QCD sum rules with nonlocal condensates from [27] is indicated by a slanted (green) rectangle.

From Fig. 3, we conclude that the BaBar data deviate from the other data sets at the 3σ level and cannot be satisfied by pion DAs based on models with only two Gegenbauer coefficients—unlike all other data sets—and hence they require (at least) a sizable coefficient a_6 or still higher coefficients.

CONCLUSIONS

It is not a trivial matter that QCD has come to use collinear factorization to describe basic exclusive processes, like the pion-photon transition form factor. This scheme has been challenged by the BaBar data because they indicate an auxetic behavior at $Q^2 > 9 \text{ GeV}^2$ that cannot be uniquely described by a known QCD mechanism. Therefore, the Belle data, which do not replicate this increase of the scaled pion-photon transition form factor, may help restoring the confidence to the standard QCD scheme, though a definitive answer requires more accurate data in the high- Q^2 range.

ACKNOWLEDGMENTS

One of us (A.V.P.) is thankful to V. Braun, and D. Melikhov for fruitful discussions during the QCD@Work Conference, 2012, Lecce, Italy. This work was supported in part by the Heisenberg–Landau Program under Grant 2012, the Russian Foundation for Fundamental Research (Grant No. 12-02-00613a), and the BRFBR–JINR Cooperation Program under contract No. F10D-002. The work of A.V.P. was supported in part by HadronPhysics2, Spanish Ministerio de Economia y Competitividad and EU FEDER under contract FPA2010-21750-C02-01, AIC10-D-000598, and GVPrometeo2009/129.

REFERENCES

1. S. J. Brodsky and G. P. Lepage, Adv. Ser. Direct. High Energy Phys. **5**, 93 (1989).
2. H. J. Behrend *et al.* [CELLO Collaboration], Z. Phys. **C49**, 401 (1991).
3. J. Gronberg *et al.* [CLEO Collaboration], Phys. Rev. **D57**, 33 (1998).
4. B. Aubert *et al.* [BaBar Collaboration], Phys. Rev. **D80**, 052002 (2009).
5. S. Uehara *et al.* [Belle Collaboration], arXiv:1205.3249 [hep-ex].
6. M. Unverzagt, J. Phys. Conf. Ser. **349**, 012015 (2012).
7. A. V. Radyushkin and R. Ruskov, Nucl. Phys. **B481**, 625 (1996).
8. A. P. Bakulev, S. V. Mikhailov, A. V. Pimikov, and N. G. Stefanis, Phys. Rev. **D84**, 034014 (2011).
9. A. P. Bakulev, S. V. Mikhailov, A. V. Pimikov, and N. G. Stefanis, Phys. Rev. **D86**, 031501(R) (2012).
10. H. R. Grigoryan and A. V. Radyushkin, Phys. Rev. **D78**, 115008 (2008).
11. A. V. Radyushkin, Phys. Rev. **D80**, 094009 (2009).
12. M. V. Polyakov, JETP Lett. **90**, 228 (2009).
13. S. Noguera and V. Vento, Eur. Phys. J. **A46**, 197 (2010).
14. H. L. L. Roberts *et al.*, Phys. Rev. **C82**, 065202 (2010).
15. S. S. Agaev *et al.*, Phys. Rev. **D83**, 054020 (2011); arXiv:1206.3968 [hep-ph].
16. S. J. Brodsky, F.-G. Cao, and G. F. de Teramond, Phys. Rev. **D84**, 033001 (2011).
17. D. Melikhov and B. Stech, Phys. Rev. **D85**, 051901 (2012).
18. I. I. Balitsky, V. M. Braun, and A. V. Kolesnichenko, Nucl. Phys. **B312**, 509 (1989).
19. A. Khodjamirian, Eur. Phys. J. **C6**, 477 (1999).
20. N. G. Stefanis, A. P. Bakulev, S. V. Mikhailov, and A. V. Pimikov, arXiv:1202.1781 [hep-ph].
21. H. Czyż, S. Ivashyn, A. Korchin, and O. Shekhovtsova, Phys. Rev. **D85**, 094010 (2012).
22. S. V. Mikhailov and N. G. Stefanis, Nucl. Phys. **B821**, 291 (2009).
23. A. P. Bakulev, S. V. Mikhailov, and N. G. Stefanis, Phys. Rev. **D67**, 074012 (2003).
24. A. V. Efremov and A. V. Radyushkin, Phys. Lett. **B94**, 245 (1980).
25. G. P. Lepage and S. J. Brodsky, Phys. Rev. **D22**, 2157 (1980).
26. E. P. Kadantseva, S. V. Mikhailov, and A. V. Radyushkin, Sov. J. Nucl. Phys. **44**, 326 (1986).
27. A. P. Bakulev, S. V. Mikhailov, and N. G. Stefanis, Phys. Lett. **B508**, 279 (2001); *ibid.* **B590**, 309(E) (2004).